Applied Acoustics 218 (2024) 109876

Contents lists available at ScienceDirect

Applied Acoustics

journal homepage: www.elsevier.com/locate/apacoust

Healthcare headset with tuneable auditory characteristics control for children with Autism spectrum disorder

Tak Chun Kwong [a,1], Huan-Ling Yuan [b,1], Steve Wai Yin Mung [e,1], Henry Kar Hang Chu [a], Chetwyn Che Hin Chan [c], Daniel Pak Kong Lun [d], Ho Man Yu [a], Li Cheng [a], Yat Sze Choy [a,*]

[a] Department of Mechanical Engineering, The Hong Kong Polytechnic University, Hong Kong, China
[b] Department of Rehabilitation Sciences, The Hong Kong Polytechnic University, Hong Kong, China
[c] Department of Psychology, The Education University of Hong Kong, Hong Kong, China
[d] Department of Electronic and Information Engineering, The Hong Kong Polytechnic University, Hong Kong, China
[e] Research and Development Office, The Education University of Hong Kong, Hong Kong, China

ARTICLE INFO

Keywords:
Autism
Electroencephalography
Pattern clustering
Noise cancellation
Sound perception

ABSTRACT

Auditory hyperreactivity is commonly observed in children with autism spectrum disorder. Autistic children perceive different sounds in their daily lives as intolerable; in certain instances, aversive behaviours are provoked in the presence of noise. Noise-cancelling headphones are often used to cope with behavioural problems related to auditory hyperreactivity in children with autism spectrum disorder. However, noise attenuation in traditional headphones is focused on the suppression of noise amplitude levels without considering the heterogeneous aural perceptions of autistic children. To design a suitable noise-control function in headphones to cater to children with autism, who have different aural perceptions, a series of aural perception and electroencephalography tests were conducted, wherein autistic children with auditory hyperreactivity listened to sounds of different frequencies and amplitudes to analyse their subjective aural responses. Suitable noise-attenuation targets were determined based on hearing perception curves that were constructed as a function of the mean aural perception ratings and noise levels using power function fitting. Subsequently, a hybrid active noise cancellation (ANC) system based on aural perception was developed and validated. The results showed that frequencies of 250 Hz and 8 kHz were rated by the majority of the children with autism as most unpleasant. The participants were partitioned into five clusters using the K-means algorithm. Each cluster was found to have its own characteristic aural perception response. Ultimately, an improvement in the aural perception response was observed when the children used this type of headset that had aural perception characteristics suitable for different clusters of children with autism.

1. Introduction

Autism spectrum disorder (ASD) is a neurodevelopmental condition characterized by deficits in social interaction and communication, and repetitive, restricted and stereotyped patterns of behaviour. It is accompanied by various sensory features such as hyper- or hypo-reactivity to sensory input, a strong need for routines, and fixated interests [1]. The global prevalence of autism is estimated to be 100 per 10,000, and it has increased in recent years. Among all the sensory modalities, one of the most commonly documented sensory sensitivity in autistic individuals is auditory hyperreactivity, which affects up to 65 % of children with autism [2].

Several studies have examined the atypical sound perception in children with autism. Rosenhall [3] evaluated the tolerability to loud sounds in autistic children. They showed that 18 % of autistic adolescents and children could not tolerate a sound pressure level of 80 dB HL. Khalfa et al. [4] investigated subjective perception of loudness using puretone for 250 Hz to 8000 Hz. Results showed that the loudness discomfort level was lower than 80 dB HL in 63 % of the children with autism compared to 27 % of the control group, and the 1000-Hz tones were perceived to be approximately 20 dB louder by the autistic group for sound intensity levels greater than 40 dB HL [4]. Lucker [5]

* Corresponding author.
E-mail address: mmyschoy@polyu.edu.hk (Y.S. Choy).
[1] These authors contributed equally to this work.

https://doi.org/10.1016/j.apacoust.2024.109876
Received 15 August 2023; Received in revised form 10 January 2024; Accepted 13 January 2024
Available online 19 January 2024
0003-682X/

investigated the tolerance of children with auditory hypersensitivity to loud sounds and the differences in auditory hyperreactivity between children with and without autism. Warbled tone and narrow-band noise at octave frequencies of 1000–8000 Hz were delivered starting from 80 dB HL, with a maximum of 110 dB HL. The study found that children with autism were less able to tolerate loud sounds above 100 dB HL compared to non-autistic children [5].

In addition to enhanced loudness perception and discomfort, children with autism may find certain sounds to be more disturbing than typical children. Kuiper [6] found that the autistic group found both tones and sirens to be significantly more stressful than typical children when they were asked to provide arousal and valence rating. Tan [7] found that children with autism display more auditory abnormalities, such as being over-distressed to certain sounds and oversensitive to those sound at low volumes. Although the aforementioned studies provided evidence of sounds that are disturbing to people with autism, there is still a lack of research on the influence of the physical properties of the sound, including the frequency and sound intensity level, on children with autism. These parameters are beneficial for determining the relationship between the dominant frequency, amplitude components, and aural sensation or behaviour.

In addition, neuroscience studies have been conducted on auditory responses in autistic children. One of these commonly used methods is electroencephalography (EEG), a non-invasive method that measures the neural signals elicited in the brain across all ages and functioning levels. Auditory event related potentials (ERPs) comprise positive and negative EEG amplitude deflections in response to sound stimuli in a time-locked manner [8]. The first positive and negative deflections at approximately 50 ms and 100 ms after the stimulus, respectively, are often measured in auditory ERP studies. Shepherd et al. [9] examined the electrophysiological responses of individuals with different noise sensitivities. Using pure tones at frequencies of 1000 Hz and 2500 Hz at a 70 dB sound pressure level, a larger first positive deflection was observed in noise-sensitive participants relative to that of the noise-resistant group. This suggests that individuals with a high noise sensitivity may have less sensory gating than noise-resistant individuals. Besides, Li et al. [10] found that changes in certain frequency bands in the EEG power spectrum components were associated with pleasant sounds. For example, the difference in alpha and beta band components in the EEG power spectrum was related to the level of comfort experienced by an individual in a soundscape.

When children with autism who are sensitive to sound perceive unpleasant auditory stimuli, not only would it result in strong reactions but it could also result in reduced engagement in important life activities and avoidance of specific environments and interactions, which influence the quality of their lives [11]. These effects could persist into adulthood. Sturrock [12] interviewed nine autistic adults and conducted qualitative study on their experiences of speech perception. It was found that there were pronounced difficulties in perceiving speeches. One of the main factors were the acoustic features of the environment such as the presence of continuous noise, overlapping sound and strong auditory distractions. Therefore, it is important to control the surrounding noise in their daily life. One common environmental noise control method involves controlling the sound propagation path, for example, by installing noise-absorbing panels [13,14] and designating a quiet zone by erecting a barrier [15]. However, this method, with a fixed noise suppression facility at one location, is unsuitable for human beings who move around and undertake activities in different locations in their daily lives. Therefore, earmuffs and portable noise-cancelling headphones are appropriate for controlling noise directly at the receiver. They provide a barrier between the ears and the external environment. The porous material in the ear-cushion can absorb noise in the high-frequency range; however, its working performance in the low-frequency region is poor. To address this problem, active noise cancellation (ANC) can be integrated into the headphones. This involves an electroacoustic system that is responsible for creating a local quiet zone through the cancellation of unwanted noise based on the principle of superposition. ANC enables the efficient attenuation of low-frequency noise, wherein passive methods tend to be bulky, and are used in many applications [16,17]. This enables implementation in equipment with small form factors, such as headphones. Rowe et al. [18] observed that autistic child having auditory hyperreactivity displayed more consistent attention to work tasks when they wore noise-cancelling headphones. Ikuta et al. [19] identified improved behavioural responses in autistic children who perceived noisy classroom sounds as intolerable with the use of noise-cancelling headphones. The aforementioned noise-cancelling headphones that use an active noise control technique are based on the suppression of the sound pressure level only, and children with autism use the same type of noise cancelling function without considering their individual aural sensations.

To design a suitable noise control function in headphones to cater to children with autism having different aural perceptions, the objectives of the study were (1) to investigate the aural response of children with autism and auditory hyperreactivity in terms of amplitude and frequency; (2) to establish an assessment method that can quantify the perception of sound of the autistic children; (3) to determine the relationship between the physical parameters of sound and the subjective aural response; and (4) to develop a suitable human perception ANC approach to effectively alleviate the adverse behaviours related to auditory hyperreactivity in children with autism.

2. Assessment

To understand the aural sensation in children with autism and the difference between them and children with typical development, the assessment of their acoustic responses was conducted in two sessions. The first session was focused on the subjective evaluation experiments, which directly reflected the subjective aural perception of different sound stimuli. The second session included physiological acoustic responses that reflected the intermediate neural response to sound excitation and its corresponding emotion.

2.1. Participants

There are two groups of children participants: typical growth children (TD) and children with autism (ASD). A total of 83 ASD participants (seventy-five males and eight females, with a mean age of 9 ± 1.7 years) and 50 TD children (thirty-eight males and nineteen females, with a mean age of 10 ± 1.4 years) were recruited by means of purposive and snowball sampling. The recruited children with autism were diagnosed with autism, autistic disorder, or Asperger's syndrome and completed the Hong Kong version of Autism Spectrum Quotient [20,21]; aged 7–12 years; and with primary education. Children were able to respond verbally using a five-point Likert scale. The normal hearing function of these children was assessed using a hearing ability test with pure tone audiometry [22]. For the hearing ability test, all the participants were screened twice for their hearing threshold at 250, 500, 1000, 2000, 3000, 4000, and 8000 Hz with three different sound-intensity hearing levels (10, 15, and 20 dB HL). Participants were asked to indicate verbally or through gestures whether they could hear a sound delivered by the headphones. The average hearing level of the children over all the measured frequencies was higher than acceptable level of 15 dB HL. In addition, these children scored 85 or higher on the Test of Nonverbal Intelligence, Fourth Edition (TONI-4) [23]. To obtain their neural responses upon acoustic excitation, the children were confirmed to have no neurological disorders. The autistic participants had also completed an auditory hyperreactivity screening using the Chinese version of the Sensory Profile [24] for auditory hyperreactivity where scores of 30 or less were defined as having auditory hyperreactivity.

2.2. Sound stimuli

To obtain the acoustic perception and aural responses of the two groups of participants, the sound stimuli were focused on tonal signals with different frequencies and amplitudes. The full set of sound stimuli comprised 36 sound tracks, with six different frequencies (0.25 kHz, 0.5 kHz, 1 kHz, 2 kHz, 4 kHz, and 8 kHz) and six different sound intensity hearing levels (30, 40, 50, 60, 70, and 78 dB HL), where dB HL is the decibels in hearing level commonly used in audiology, wherein 0 dB HL is the average hearing threshold in dB sound pressure level for the average, normal-hearing listener. The sound stimuli were adjusted to sound levels in dB HL to mitigate the differences in human ear's response to low and high frequencies, such that the effect of frequency on the aural perception under the same perceived sound level could be observed. These six centre octave frequencies cover almost the entire frequency range of environmental sounds in the community and frequency range of natural sound in terms of sound energy [25]. Each tonal sound with a corresponding amplitude was generated for a duration of 1 s and a 20-ms onset/offset ramp, as shown in Fig. 1(a). The entire set of acoustic stimuli with the aforementioned frequencies and amplitudes was repeated thrice. The equipment used for the sound stimuli presentation was calibrated using a head and torso simulator in a listening chamber with low background noise to ensure the accurate delivery of sound stimuli [25]. The calibration setup is presented in Fig. 1(b).

2.3. Procedure

The subjective aural perception of the children was evaluated in a soundproof chamber. During the experiment, sound stimuli were played using a computer connected to Bose QC35II headphones with an audio amplifier. The experiment control software E-Prime 2.0 was utilised to create a randomised sound stimuli sequence for each participant. This enabled researchers to record participants' responses using a response pad without them knowing the sound stimuli sequence in advance. In addition, the software allows researchers to insert an interstimulus interval (a time interval with silence in this experiment) with varying durations based on the participants' responses after each sound stimuli. The purpose of the interstimulus intervals and durations is discussed in detail below. The procedure for presenting each sound stimulus was as follows. Before the presentation of each sound stimulus, a black fixation cross appeared at the centre of the screen to capture the participant's attention. After the sound was played, each participant was presented with a five-point Likert scale along with the corresponding emoticon, as shown in Fig. 2. The Likert scale was designed as a bipolar scale to capture both the pleasant and unpleasant feelings of the participants when listening to sound stimuli. The children were asked to verbally rate how much they liked or disliked the sound. The ratings were + 2 representing 'strongly like' with a broadly smiling face emoticon, +1 representing 'like' with a smiling face emoticon, 0 representing 'neutral' with a neutral face emoticon, −1 representing 'dislike' with a sad face emoticon, and − 2 representing 'strongly dislike' with a very sad face emoticon on the display. If a participant did not hear a sound, the researcher would repeat it. The interstimulus intervals were between 2 and 10 s, depending on the participant's response, to avoid habituation effects. For trials with ratings of − 1 (dislike) or − 2 (strongly dislike), the intervals varied between 8 and 10 s. The interval was 5 s for trials with a rating of 0 (neutral). For trials with ratings of + 1 (like) or + 2 (strongly like), the intervals varied between 2 and 4 s. The entire set of sound stimuli consisted of 36 sound stimuli, which were repeated thrice at random to check the repeatability. The total experiment duration was approximately 30 min.

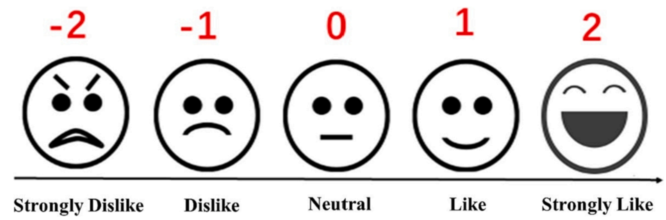

Fig. 2. Five-point Likert scale with the corresponding emoticon adopted in the aural perception test.

2.4. Electroencephalography (EEG) test

To scrutinise the reliability and consistency of the acoustics perception response by the participants to the sound stimuli, the neural responses of the participants with regard to the auditory stimuli were also measured through an EEG test. The sound stimuli in this section were focused on 18 soundtracks comprising the same frequencies (250, 500, 1000, 2000, 4000, and 8000 Hz) in the aural perception test described in Section 2.3 and three different sound intensity hearing levels of 40, 60, and 78 dB HL. The quantity of acoustic stimuli in the EEG test was less than that in the acoustics perception response section because the time required cannot be too long for children with autism to endure. All sound stimuli were generated through a Panasonic RP-HD5 headphone controlled by the E-Prime 2.0 software with a duration of 200 ms and a 20-ms onset/offset ramp. In this experiment, the participants sat in a comfortable chair in a soundproof, electrically shielded, and dimly lit chamber, as shown in Fig. 3(a). During the entire experimental process, the children were instructed not to pay attention to the sound and watch the silent movie of their choice. They were asked to remain still and try to blink less frequently. As shown in Fig. 3(b), three EEG electrodes, denoted as Fz, Cz, and Pz, were placed in the frontal,

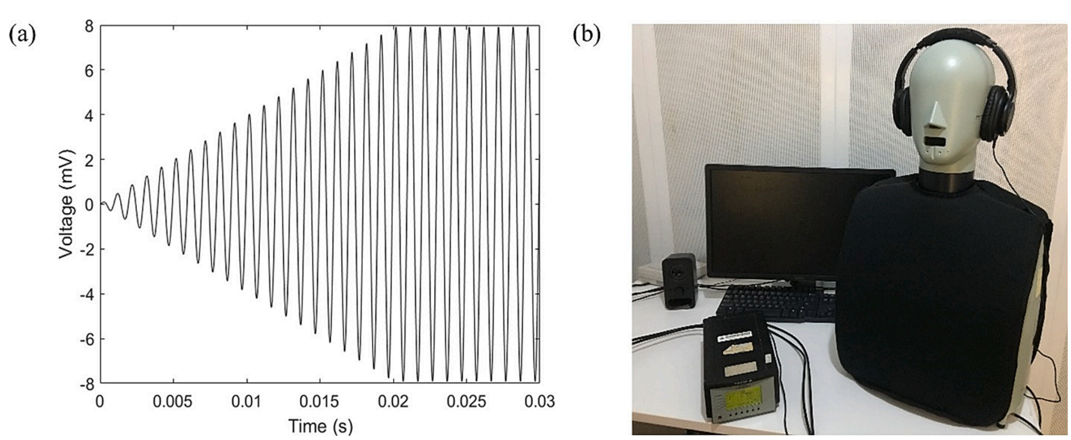

Fig. 1. (a) Example of tonal sound with duration of 1 s and 20 ms onset/offset ramp; (b) Calibration setup of sound stimuli presentation system.

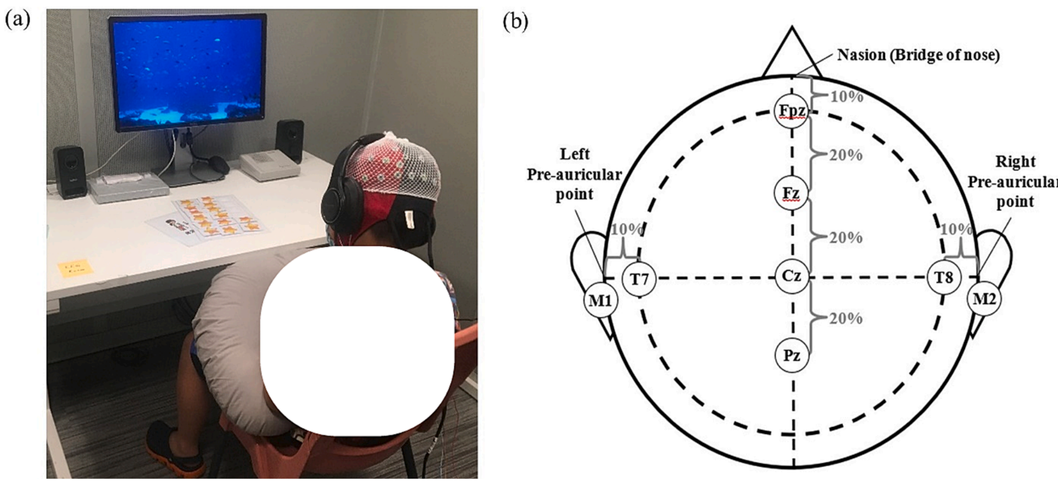

Fig. 3. (a) Participant of the EEG experiment wearing the EEG cap to record the raw EEG signals while listening to sound stimuli from the headphone and (b) EEG electrode position in the EEG test.

central, and parietal positions, respectively, along the midline sagittal plane of the head. Another two electrodes are situated on the left and right sides of the temple of the head and are denoted as T7 and T8, respectively. The brain wave signal captured by electrodes placed on the waveguard^{TM} EEG cap was recorded by the ANT-Neuro eego^{TM} mylab amplifier. The electrode located on the left mastoid (M1) was regarded as the reference, and the frontopolar midline electrode was regarded as the ground. The electrode located on the right mastoid (M2) was recorded for re-referencing in the offline processing stage. Four additional Ag/AgCl cup electrodes were placed near the eye to monitor the eye movement. The electrodes were fabricated from sintered Ag/AgCl by COMPUMEDICS®. The electrode impedances were maintained below 5 kΩ. The EEG was sampled at a rate of 1 kHz for the entire session. Each sound stimulus was generated 40 times in a randomised pattern for each participant. The interstimulus interval was jittered between 2 and 3 s. To mitigate the effect of fatigue and emotion on the EEG data, measures were implemented such as visualization of the experiment design using illustrations, as well as reinforcement of feedback by rewarding them token for exchange of gifts after the experiment after the completion of the tasks of experiment similar to the method adopted in previous study [26]. In addition, children were granted a break whenever they feel tired. The entire test consisted of 720 trials and lasted approximately 55 min.

The recorded EEG data were imported into MATLAB for offline processing and analysis to investigate the relationship between the electrophysiological and aural perception responses to auditory stimuli. The data were re-referenced to the averages of the left and right mastoids. This provides a symmetrical reference that is not partial to one of the hemispheres. The equation for the referencing procedure is shown below, using channel Fz as an example. This referencing procedure was repeated for each EEG channel recorded. Let V_{Fz}, V_{M1} and V_{M2} be the absolute voltages at sites Fz, M1, and M2, respectively. Let V_{Fz}'' be the voltage at site Fz after the re-referencing.

$$V_{Fz}'' = V_{Fz} - \frac{1}{2}(V_{M2} + V_{M1}) \tag{1}$$

The data were filtered using a windowed-sinc filter as a notch filter at 50 Hz with a filter kernel length of 1650 points to remove line noise. The filter kernel is given by $h[i] = \sin(2\pi f_c i)/i\pi$. Another windowed-sinc filter with a cutoff frequency of 40 Hz and a filter kernel length of 3300 points was used as a low-pass filter to mitigate high-frequency noise such as muscle artefacts. A windowed-sinc filter with a cutoff frequency of 1 Hz and a filter kernel length of 3300 points was then utilised as a high-pass filter to minimise the low-frequency noise possibly caused by body movement, improper skin-electrode contact, and respiration. Bad channels and noisy segments were removed and corrected using an artefact subspace reconstruction approach [27]. To investigate the electrophysiological response elicited in response to the sound stimulus, specific time windows around the onset of each sound stimulus were extracted from continuous EEG recordings. These time windows were time-locked to the sound stimuli and called epochs. In this study, the continuous EEG data were separated into 600-ms epochs with 100 ms before each stimulus onset and 500 ms after each stimulus onset. The 100-ms time intervals before each stimulus onset (baseline period) were used for realizing baseline correction, where the mean value of the EEG data in these 100-ms pre-stimulus time intervals was computed and then subtracted from every time point of the baseline period and the post-stimulus interval for each epoch. Baseline correction was performed to reduce the effect of baseline differences between epochs that are not meaningful for interpretation and may have biased the data analysis results. Epochs with a signal amplitude exceeding $\pm$ 90 μV in any channel are excluded. Epochs corresponding to the same sound stimulus were averaged such that the spontaneous background EEG activity, such as noise, was averaged out, leaving the time-locked EEG response elicited by the sound stimulus distinct from the background. This averaging procedure was repeated for each sound stimulus, and the resulting time-locked EEG responses were exported. To ensure the reliability of the results, only data with components in the period described by traditional slow-wave cortical auditory evoked potentials were included in the analysis. These components are characteristic deflections that occur around specific peak latencies, where the peak latency is measured using the stimulus onset as the reference point (i.e. 0 ms begins at stimulus onset). In this study, the first and second positive peaks are denoted as P1 and P2, with peak latencies of approximately 50 ms and in the 175–200 ms range, respectively. The first trough point, denoted as N1, is a prominent negative wave peaking at approximately 100 ms. The peak amplitudes and latencies of the P1, N1, and P2 components in the temporal signals of event-related electrical potentials were used to quantify the neural responses of the participants toward the auditory stimuli. These response characteristics are substantially influenced by the physical attributes of the provocation, such as the duration of sound stimuli, rise time (time taken by the sound signal from silence to peak amplitude), sound intensity level, interstimulus interval, and stimulus features [28,29]. To identify these three components, we focused on searching for the peaks of P1 and P2 in the periods 20–120 ms and 150–250 ms, respectively. For the first trough point, the N1 component, the search window was focused from 70 ms to 150 ms. In the analysis, a peak was identified as the data point with the maximum positive amplitude for P1 and P2 and the data point with the maximum negative amplitude for N1 within the search window. The peak amplitude value is measured as the average magnitude of data ± 1 ms around the peak, which is the average value of the peak and the values of data 1 ms before and after the peak. The peak amplitudes and latencies of the P1, N1, and P2 components were investigated.

3. Results and discussions

To enhance the quality of data, participants were included in the analysis only if they displayed consistent and reliable responses in both the aural perception and EEG tests. In the aural perception test, the consistency of the participants across three repeated assessments of the aural perception test was evaluated using the one-way random effects, absolute agreement, multiple measurements intraclass correlation coefficient (ICC). McGraw and Wong's study [30] indicated that when the p-value of the ICC was less than or equal to 0.05, participants' consistency in the three repeated tests was significantly higher. Individuals with an ICC value of less than or equal to 0.38 ($p > 0.05$) were therefore deemed inconsistent and excluded in the data analysis. Furthermore, after data pre-processing and cleaning, participants with fewer than 540 epochs (less than 75 % valid epochs) were left out of the screening process for reliable subjects. Consequently, 33 ASD and 12 TD participants were excluded. In total, 50 ASD and 38 TD participants aged 7–12 years were included in the analysis.

3.1. Aural perception test

The score of the aural perception test response were adjusted to a positive number from (−2 to + 2) to (1 to 5), wherein the adjusted scale rating 1 represents "strongly dislike" and rating 5 represents "strongly like". This scale adjustment was performed for ease of data analysis and interpretation of aural perception and electrophysiological responses to sound stimuli. For each participant, the responses to each sound stimulus across three repeated assessments in the aural perception test were averaged to obtain a mean score. This resulted in 36 mean scores for each participant. These scores represent the individual variation patterns of each participant and were adopted for further analysis in the following sections. In addition, the mean scores for all 36 sound stimuli were averaged to obtain a mean score for each participant. This mean score measured the aural perception of the participants, while considering their responses to 36 sound stimuli with a uniform weighting. A lower score indicated a greater dislike toward the sound stimuli, while a higher score indicated a greater liking for the sound stimuli. The mean score of all the TD participants were averaged to be used as the cutoff for categorisation into two groups of children with autism. Those with a score higher than the TD cutoff were classified as ASD group 1, whereas those with a score less than the TD cutoff were classified as ASD group 2. Thirty-eight ASD children were included in group 1 while twelve children were included in group 2.

The mean scores of the two ASD groups and the TD group based on the aural perception experiment are presented in Fig. 4. Generally speaking, the mean score of the ASD group 1 (dashed line) was higher than that of TD at all the frequencies and sound intensity hearing levels, except at 250 Hz at 78 dB HL. At lower sound intensity hearing levels, such as 30 and 40 dB HL, the mean score increased in the frequency range of 250 Hz to 1 kHz, then decreased toward the frequency of 8 kHz. This indicates that they dislike frequencies at 250 Hz and 8 kHz more and are generally willing to listen to sounds in the mid-range frequency of approximately 1 kHz. At 50 and 60 dB HL, the differences between the mean scores at 250 Hz and 8 kHz versus those at other frequencies became more noticeable. At 70 dB HL, the profile of the mean score variation against frequency is similar to that at 50 and 60 dB HL, and the mean score at almost all the frequencies is lower than 3, which indicates that they dislike these sounds. The mean score curve of ASD group 1 was higher for the majority of the presented sound stimuli than for the TD participants. This result indicates that ASD group 1 in general had less annoyance towards the presented stimuli. ASD group 2 (dash-dotted line) had a relatively lower mean score for all the sound stimuli compared to the TD group, but manifested a similar variation pattern to the TD group. At 30 and 40 dB HL, the responses resembled the TD

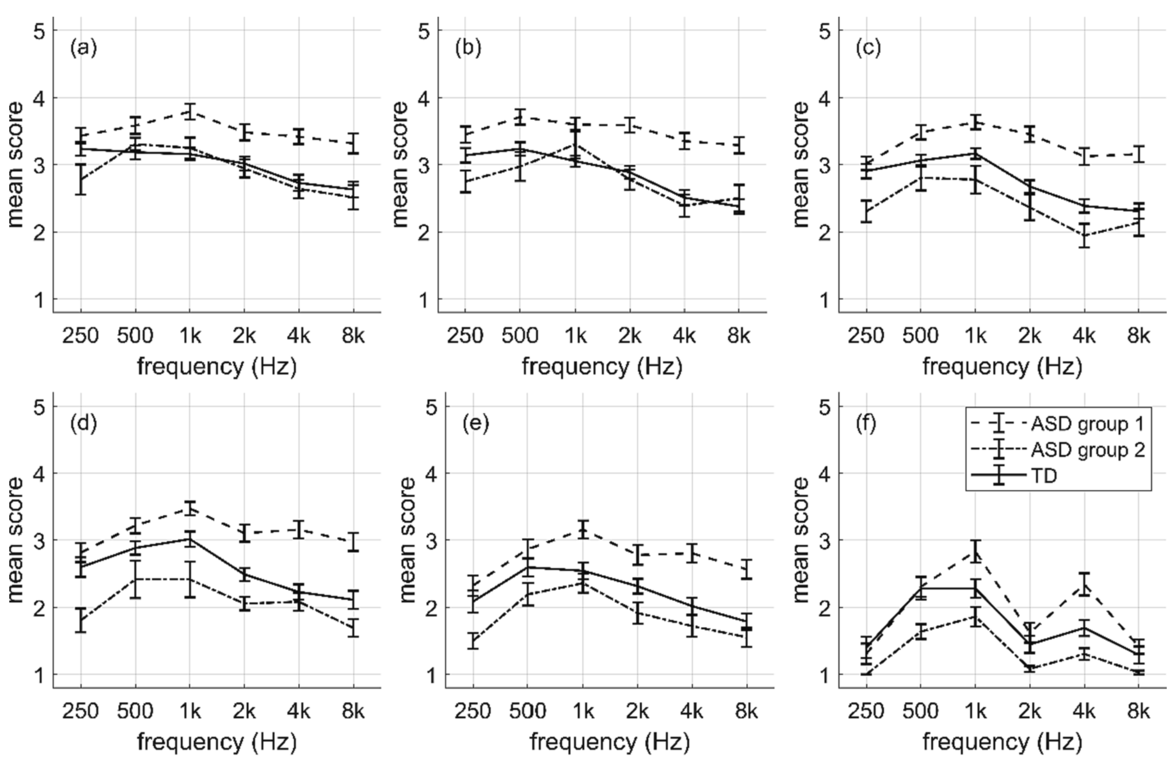

Fig. 4. Aural perception mean score with grouping at different sound intensity hearing levels, (a) 30 dBHL; (b) 40 dBHL; (c) 50 dBHL; (d) 60 dBHL; (e) 70 dBHL; (f) 78 dBHL.

responses, except for a substantially lower mean score at a frequency of 250 Hz. At 50–70 dB HL, this group of children with autism exhibited an unpleasant response to all the sound stimuli, and a lower mean score was observed at all frequencies compared with the TD group.

3.2. Relationship between aural perception response and EEG subject to the tonal sound

To validate the subjective aural perception, the relationship between this response and the EEG results was investigated. Spearman's correlation analysis was used to analyse their correlations. The results of ASD children combining groups 1 and 2 and those of TD children are listed in Table 1. In the ASD group, there were significant correlations between aural perception and absolute N1 peak amplitude and P1 and P2 peak latencies at specific EEG channels. The correlation coefficients for N1 peak amplitude ranged from -0.118 to -0.149, $p < 0.01$, and for P1 and P2 peak latencies, coefficients ranged from 0.122 to 0.194, $p < 0.01$. In the TD group, significant correlations were found between aural perception and absolute N1 peak amplitude and P1 and P2 peak latencies across multiple EEG channels, with correlation coefficients ranging from -0.103 to -0.270, $p < 0.01$ and 0.109 to 0.170, $p < 0.01$, respectively. Aural perception is a subjective evaluation of the sound provided by participants, whereas the neural response displays an objective reaction to sound. The correlation between these two responses suggests that the mean aural perception score is indicative of the participants' subjective perception of the presented sound stimuli. For both the ASD and TD groups, the absolute N1 peak amplitude generally exhibited a better association with the aural perception response. This indicates that the N1 peak amplitude may be a suitable candidate for quantifying children's neural responses to sound stimuli. In general, the higher the sound intensity hearing level, the higher the absolute peak amplitude of the components N1 and lower was the peak latency.

Fig. 5 presents a comparison of the peak amplitude and peak latency N1 components at channel T8 in the TD and ASD groups. Channel T8 was selected because relatively high correlation coefficient values were observed in this channel in both the ASD and TD groups. The results of the TD participants provide a baseline for how the frequency and sound intensity hearing levels would affect the peak amplitude and peak latency of the components. In general, the higher the sound intensity hearing level, the higher the absolute peak amplitude of the components. In addition, the higher the sound intensity hearing level, the lower was the peak latency. This is clearly observed in the N1 component. When looking at the N1 peak amplitude, the TD group had an overall smaller magnitude than the ASD group. These differences in ERP responses between TD and ASD group have other potential applications such as serving as parameter for diagnosing autism in children using their auditory responses with artificial neural networks [31]. A detailed analysis of the ERP data will be conducted in another study.

3.3. Clustering of ASD children

Many surveys have found that children with autism have distinct acoustic responses and individual acoustic sensitivities to different types of sound sources [32]. Some children may like a particular type of sound, but others find it unpleasant. This suggests that the physical properties of sounds that provoke problematic behaviour vary from person to person. Therefore, a headset with the same noise-control strategy and algorithm is inappropriate for children with different aural perception responses and sensations. Therefore, it is essential to provide customised noise control for autistic children with different frequency profiles. To achieve this, a clustering analysis is conducted to cluster children with autism into different subgroups based on their aural perception, and each group will have a similar frequency profile.

3.3.1. Clustering algorithms and cluster validation indices

There are two commonly used clustering algorithm such as prototype-based clustering and hierarchical clustering depending on the nature of grouping mechanism. One of the methods under prototype-based clustering is K-means clustering which is widely adopted as partition algorithm [33]. It is a method of vector quantization that is used to partition the certain number of participants into k clusters in which each participant belongs to the cluster with the nearest mean value or centroid. This method requires the number of clusters (K), cluster initialization and the distance metric as input parameters. Let $X = \{x_i\}, i = 1, ..., n$ be the dataset to be clustered into a set of K clusters where x_i is a vector of mean aural perception scores of the i th ASD children and n is the total number of ASD children adopted in analysis. Let $C = \{c_k\}$ be the set of clusters, $k = 1, ..., K$ be the number of clusters to be formed and μ_k be the mean of cluster c_k. The squared error between μ_k and the points in cluster c_k is defined as,

$$J(c_k) = \sum_{x_i \in c_k} \|x_i - \mu_k\|^2 \tag{2}$$

The goal of k-means is to minimize the sum of squared error (SSE) over all K clusters,

$$J(c_k) = \sum_{k=1}^{K} \sum_{x_i \in c_k} \|x_i - \mu_k\|^2 \tag{3}$$

and finds a partition such that the squared error between the empirical mean of a cluster and the data points in the cluster is minimized. After the parameter K is decided, the k-means algorithm begins by initializing K randomly selected vector of mean aural perception scores in the dataset as the initial cluster centres (μ_k). For each ASD participant, the Euclidean distance between the vector of mean aural perception scores and all cluster centres are calculated. The ASD participant is assigned to the cluster with the smallest Euclidean distance. When all ASD participants are assigned to a cluster, the cluster centres are recomputed using

Table 1
Spearman correlation between ERP component response and ratings in aural perception test.

ASD	Parameters	Fz	T7	Cz	T8	Pz
	Absolute P1 peak amplitude and rating	−0.047	0.060	0.001	−0.030	0.016
	Absolute N1 peak amplitude and rating	−0.099**	−0.133**	−0.125**	−0.149**	−0.118**
	Absolute P2 peak amplitude and rating	0.005	0.099**	−0.054	0.055	−0.043
	P1 peak latency and rating	0.132**	0.048	0.148**	0.086*	0.122**
	N1 peak latency and rating	0.024	0.077*	0.107**	0.074*	0.108**
	P2 peak latency and rating	0.135**	0.030	0.194**	0.003	0.179**
TD	Absolute P1 peak amplitude and rating	0.043	−0.032	0.020	−0.065	0.005
	Absolute N1 peak amplitude and rating	−0.103**	−0.230**	−0.161**	−0.270**	−0.165**
	Absolute P2 peak amplitude and rating	0.037	0.018	−0.096*	0.000	−0.117**
	P1 peak latency and rating	0.170**	0.109**	0.136**	0.057	0.151**
	N1 peak latency and rating	0.059	0.087*	0.100**	0.094*	0.098*
	P2 peak latency and rating	−0.018	0.091*	0.076*	0.020	0.072

*Correlation is significant at the 0.05 level (2-tailed).
**Correlation is significant at the 0.01 level (2-tailed).

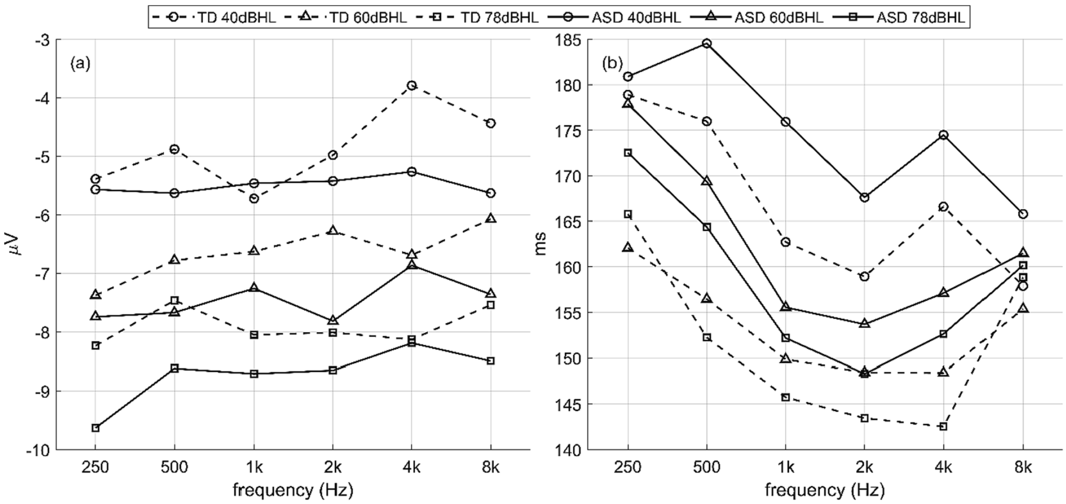

Fig. 5. Comparison of (a) peak amplitude and (b) peak latency of N1 components at channel T8 of TD and ASD groups.

the current cluster memberships. Then, the process of calculating the Euclidean distance between ASD participants and cluster centres are repeated until there are no changes in cluster assignment for all ASD participants [34]. The block diagram of K-means clustering algorithm is shown in Fig. 6.

Among the input parameters, the most critical is the number of clusters K. Currently, there is no perfect mathematical criterion for determining K. A typical heuristic for selecting K is to run the algorithm independently for different values of K and select a partition that appears to be the most meaningful solution to the problem. This approach was adopted in the current study, and the method used to select K was based on cluster validation indices.

Another input is the cluster initialisation. As K-means converges only to local minima, different initialisations can result in different clustering solutions. To overcome this problem, each number of clusters was initialised using 10,000 different initial centroid positions. This number of initialisations was selected because it provided a stable cluster solution and membership assignment in the current cluster analysis across different values of K. Subsequently, the partition with the smallest sum of squared errors was selected.

Another approach for analysing the current data is the use of agglomerative hierarchical algorithms (HCAs). This analysis involves building a hierarchy of clusters using the 'bottom-up' approach. It begins with each data point as a separate cluster and merges them into successively larger clusters until all the data are grouped into one large cluster. At each clustering step, the clusters having the smallest distance are joined together, and there are multiple methods of determining the distance between two clusters, which is referred to as a linkage. Several indicators can be used to examine (or determine) how to combine or split the clusters. For example, an average linkage measures the cluster distance as the average of all pairwise distances between data points in two clusters and Ward's linkage, which is based on the Euclidean distance between two cluster centroids multiplied by a factor. The closest pair of clusters computed using this method results in the smallest increase in the total SSE of the dataset. On comparing these linkage methods, Ward's linkage and the average linkage are generally more effective in capturing the clustering structure than the single linkage and complete linkage [35]. Therefore, the average linkage and Ward's linkage were used in the agglomerative hierarchical clustering algorithm. The silhouette index, Calinski–Harabasz index, and Davies–Bouldin index were used in this study select the appropriate clustering algorithm and optimal number of clusters because they were demonstrated to be some of the best-performing cluster validation indices in both artificial and real datasets [36]. These three indices provided better results, even in datasets with often problematic features such as high dimensionality, density asymmetry, and cluster overlap, which might also be present in our dataset.

3.3.2. *Clustering approach and partition result analysis*

A comparison of the clustering results of the three methods is presented in Table 2, which displays the cluster membership assignments of the selected K. Clustering methods are distributed in rows, whereas individual clusters are distributed in columns. Among the three clustering methods, only the HCA–average linkage tended to form a large cluster that included the majority of the participants and a few small clusters that included one to four members, regardless of the value of K. Because the aim of performing clustering is to group participants with similar frequency profiles, the cluster solution should not comprise a single cluster that includes almost all the participants, especially those with the heterogeneous aural perception responses revealed in Section 3.1. Thus, this solution is unsuitable for the current purposes. In the other two algorithms, the partitions were of similar size. The results of the cluster validation indices are presented in Fig. 7. In the case of the silhouette and Calinski–Harabasz indices, a better partition is indicated by a higher value, while in that of the Davies–Bouldin index, a lower value indicates a better partition. As suggested by the cluster validation indices, the K-means algorithm exhibits a slightly better performance than the HCA–Ward's linkage, and thus, the cluster solution of the former was selected. For the number of clusters to be formed, K = 5 was suggested by two of the three cluster validation indices as the best cluster assignment. Therefore, the ASD group was split into five clusters based on the results of the K-means clustering algorithm.

Based on the K-means clustering approach, the characteristics of the clustered group of children with autism with corresponding frequency profiles at different dB HL were investigated. Fig. 8 shows that the first cluster (ASD C1) rated frequencies of 4 kHz and 8 kHz as unpleasant at low sound intensity hearing levels, while frequencies of 250 Hz, 500 Hz, and 2 kHz were rated as neutral, and 1 kHz was rated as like. At higher sound intensity hearing levels, all frequencies were rated as unpleasant, with 250 Hz, 4 kHz, and 8 kHz being the most unpleasant. The second cluster (ASD C2) rated frequencies as neutral or similar at low sound intensity hearing levels, and rated 250 Hz and 8 kHz as unpleasant at 60 dB HL, 2 kHz and 4 kHz as unpleasant at 70 dB HL, and all frequencies as dislike at the highest sound intensity hearing level. The third cluster (ASD C3) rated all sounds above a score of 2 (dislike), except for 8 kHz at certain sound intensity hearing levels. The fourth cluster (ASD C4) rated frequencies as neutral or like at low sound intensity hearing levels, and rated 250 Hz, 500 Hz, and 2 kHz as unpleasant at 60 dB HL, and all frequencies as dislike at higher sound intensity hearing levels. The fifth cluster (ASD C5) rated most frequencies as like, with 250 Hz being the

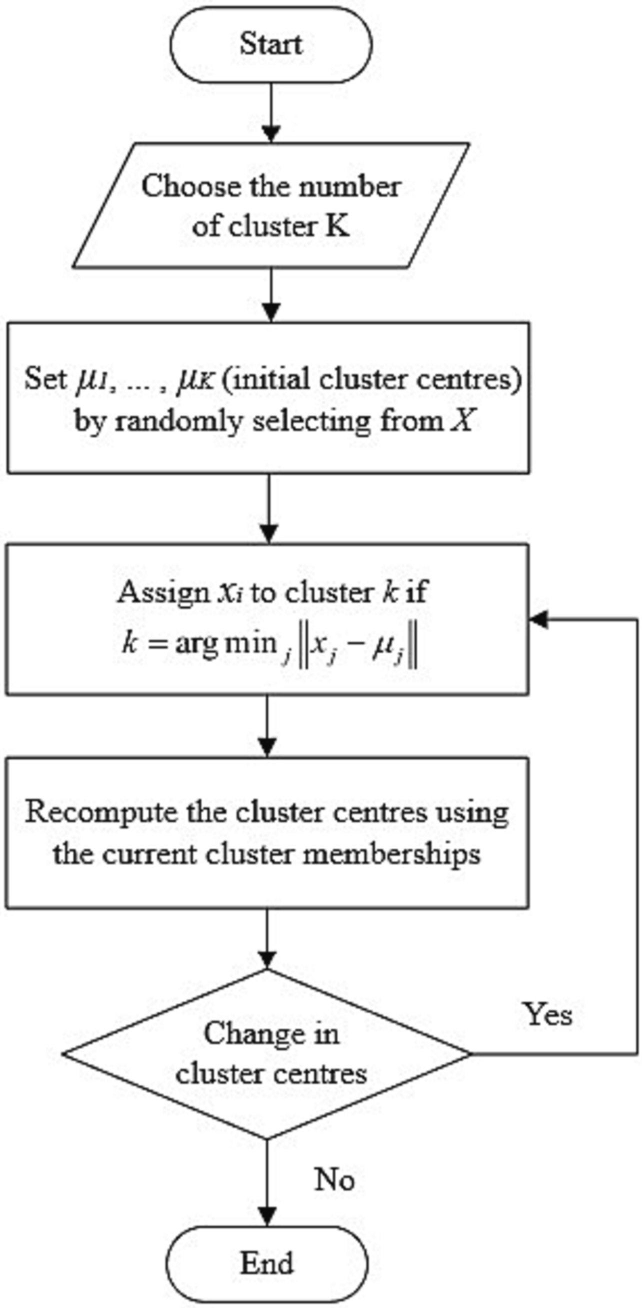

Fig. 6. K-means clustering algorithm block diagram.

only frequency rated as dislike at higher sound intensity hearing levels.

For all the clusters, the frequencies that triggered the most unpleasant feeling at a higher sound intensity hearing level were 250 Hz and 8 kHz, followed by the frequency of 2 kHz as the second most unpleasant one. At the other sound intensity hearing levels, the aural perception responses from the different groups had their own characteristics. This supports the need for customised noise control that addresses the specific annoying frequencies for each group. In addition, the magnitude of noise reduction that could result in a neutral rating for the perceived sound at the presented frequencies differed from group to group, with some requiring a more drastic reduction and others preferring a moderate level. Therefore, it is vital to consider these varied responses when designing noise-control methods for autistic children.

3.4. Hearing perception curves

To provide noise control specified for the heterogeneous needs of autistic children, the hearing perception curves for each corresponding subgroup were plotted based on the findings in Section 3.3. As the ASD group had aural perception response profiles that were different from those of the TD group, the noise control strategy was focused on providing a suitable noise control algorithm to cancel the incoming noise such that the ASD children would have a neutral response to the resultant sound. Fig. 9(a) presents the aural perception ratings against the dB HL at different frequencies. To achieve a neutral response (e.g. the dashed line in Fig. 9(aiii)) as a criterion, we must investigate the level of noise reduction required at each frequency. In this regard, a power function curve fitting with the mean aural perception rating and sound intensity hearing level as variables was performed. The fitted curve was used to estimate the mean aural perception rating between the sound intensity hearing levels tested at each frequency in the aural perception test. The power function is in the form of $y_i = a(x_i^b) + c$, where y_i is the ith mean perception rating in a specific frequency, x_i is the ith intensity level in a specific frequency, and a, b, c are the coefficients to be determined. The best-fitting curve was determined using the nonlinear least-squares method by selecting the best fit with the least sum of square errors. The power function was selected because the aural perception rating is inversely proportional to the presented sound intensity hearing level. As the sound intensity hearing level decreased, the change in the aural perception rating generally decreased. Using the hearing perception curve, it was possible to estimate the noise attenuation required to induce a neutral feeling at individual frequencies, given the noise level presented to the participant. As illustrated in Fig. 9 (aiii), to calculate the required noise reduction at a specific frequency, the sound intensity hearing level that presents a neutral feeling was first determined using the hearing perception curve (60 dB HL). The required noise attenuation level is given by the difference between the sound intensity hearing level and the noise level (78 dB HL – 60 dB HL = 18 dB HL). This provided the target curve at octave frequencies ranging from 250 to 8000 Hz for the tuning noise cancellation that is catered to hearing perception in children with autism. Fig. 9(a) and (b) present examples of the hearing perception curve along with the aural perception ratings and the resulting target curves for noise cancellation,

3.5. Active noise control (ANC) system in noise-cancellation headphone

Noise-cancelling headphones are commonly used by children with autism and auditory hyperreactivity to reduce their exposure to noise and its negative effects. Commercially available noise-cancelling headphones allow users to alter the overall noise-cancelling function by adjusting the level of noise cancellation applied by the headphones [37]. This allows users to vary the overall sound pressure level reduction. Till date, little effort has been focused on designing a noise-control strategy based on the human perception response curve, which is expressed as a function of the acoustic magnitude and frequency. Our results showed that frequency is also a component that substantially affects the aural perception of autistic children with auditory hyperreactivity; thus, the ability to tune the frequency response of the noise-cancelling function, in addition to intensity, would be more beneficial to them. To develop an ANC algorithm to ease aversive behaviours related to auditory hyperreactivity in children with autism, the frequency response and level of noise cancellation were tuned based on the results of the aural perception test. The objective of the ANC algorithm is to achieve noise cancellation such that children with autism can perceive incoming noise with a neutral feeling, thus minimising the effect of incoming disturbing noise on their behaviours. A block diagram of the ANC system with the proposed function is presented in Fig. 10. The incoming noise, which can be considered as the primary noise *X(z)*, was measured using the reference microphone of the headphone. This noise travels along the

Table 2
Cluster membership assignments from the clustering algorithms: K-Means, HCA–Average linkage, and HCA–Ward's linkage; K = 3 to 6.

K = 3	Cluster 1	Cluster 2				Cluster 3
K-Means	30	15				5
HCA-Average linkage	1	4				45
HCA-Ward's linkage	15	30				5
K = 4	**Cluster 1**	**Cluster 2**		**Cluster 3**		**Cluster 4**
K-Means	6	5		23		16
HCA-Average linkage	1	3		1		45
HCA-Ward's linkage	4	26		15		5
K = 5	**Cluster 1**	**Cluster 2**		**Cluster 3**	**Cluster 4**	**Cluster 5**
K-Means	16	23		1	6	4
HCA-Average linkage	1	44		1	3	1
HCA-Ward's linkage	1	4		4	26	15
K = 6	**Cluster 1**	**Cluster 2**	**Cluster 3**	**Cluster 4**	**Cluster 5**	**Cluster 6**
K-Means	6	18	7	14	4	4
HCA-Average linkage	4	40	1	1	3	1
HCA-Ward's linkage	6	20	1	4	4	15

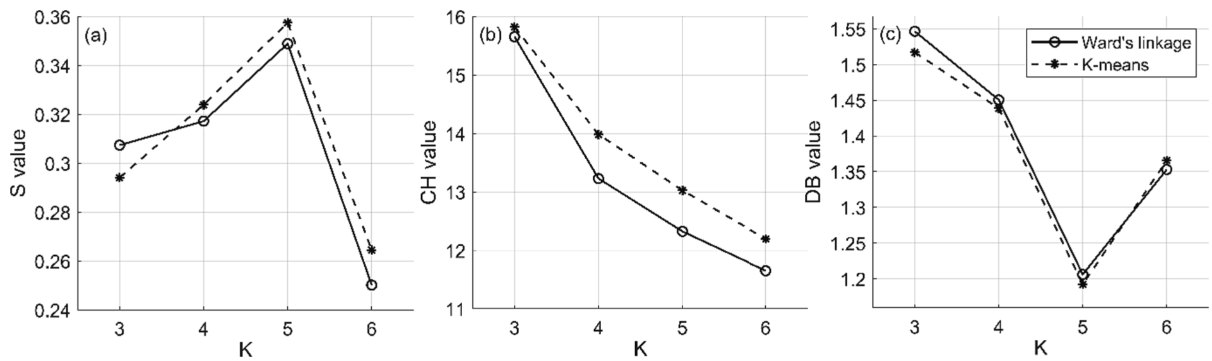

Fig. 7. Results of cluster validation indices with the three clustering methods with K of 3–6: (a) Silhouette index; (b) Calinski–Harabasz index; (c) Davies–Bouldin index.

primary path *P(z)* from the exterior of the earcup into its interior. The residual noise *D(z)* represents the noise that remains after noise is absorbed by the ear cushion. The system outputs a cancellation signal *Y(z)* that travels through the secondary path (*S(z)*), which includes the electronic software and hardware components, as well as the acoustic path from the loudspeaker to the error microphone. This combines the residual noise and results in the cancellation of both the noises based on the principle of superposition. Commonly used adaptive noise control systems include feedback, feedforward, and hybrid control [38]. In feedback control, the cancellation signal is produced using the error microphone signal because feedback and reference signals are not required. However, its active-attenuation performance is limited by the resonant behaviour of the earcup cavity, which forces low feedback gains. In general, feedforward control can result in better performance than feedback control if a good reference signal is available and the system is efficient in satisfying causality; else, it could suffer from stability or performance deficiencies caused by limited tolerance to gain error. The hybrid control system maintains the advantages of the feedforward and feedback control systems, overcomes the instability of the feedback system, and compensates for the poor adaptability of the feedforward system to primary noise [39]. Therefore, a hybrid system is used in this study. The objective of the adaptive filter *W(z)* is to minimise the error signal *E(z)* measured by the error microphone in the headphones with reference to the hearing perception curve. The error signal is the resulting signal of the residual noise added to the cancellation signal; thus, the amount of noise reduction provided by the ANC system at the frequency of interest can be obtained by comparing the sound pressure level difference between the primary signal and error signal in the frequency domain. Noise reduction measurements at these frequencies were compared with the target noise reduction level. If the error microphone measurement level deviates by more than ± 1.5 dB from the target level at any frequency in interest, the coefficient in *W(z)* is varied in order to achieve the target noise reduction level.

3.6. Validation of aural perception-based noise control method

A validation test was conducted to examine the noise cancellation tuning performance based on the hearing-perception curve. The sound-presentation system, experimental environment, and procedures were similar to that of the aural perception test described in Section 3.1, except that the presented auditory stimuli were processed with noise attenuation according to the target curve. Twenty-one participants recruited for the study were invited to participate in the validation. A comparison of the aural perception responses from ASD children subject to the original and processed sound stimuli is presented in Fig. 11. The results indicate that the proposed tuneable sonic perception method is effective especially for moderate-to-high noise levels. The aim of the target noise-reduction levels is to provide a neutral feeling instead of achieving maximum noise reduction in the current project. Now we found that the perception score ratings remained close to the target of a neutral feeling (score of 3) across the frequencies and sound intensity hearing levels tested with the use of the proposed noise control method. A slightly larger deviation was observed at the frequency of 250 Hz and 8 kHz compared to the other frequencies at 78 dB HL; however, we still observed an improvement in the aural perception response after applying the noise control. Similarly, better aural perception responses were observed for all the frequencies in the range of 60–78 dB HL, except for the frequency of 1 kHz. This might be related to the effective frequency range of the active and passive noise control methods. Active noise cancellation is more effective in the low-frequency range, such as at frequencies of 250 and 500 Hz. The level of noise cancellation became increasingly limited when the noise frequency approached 1 kHz.

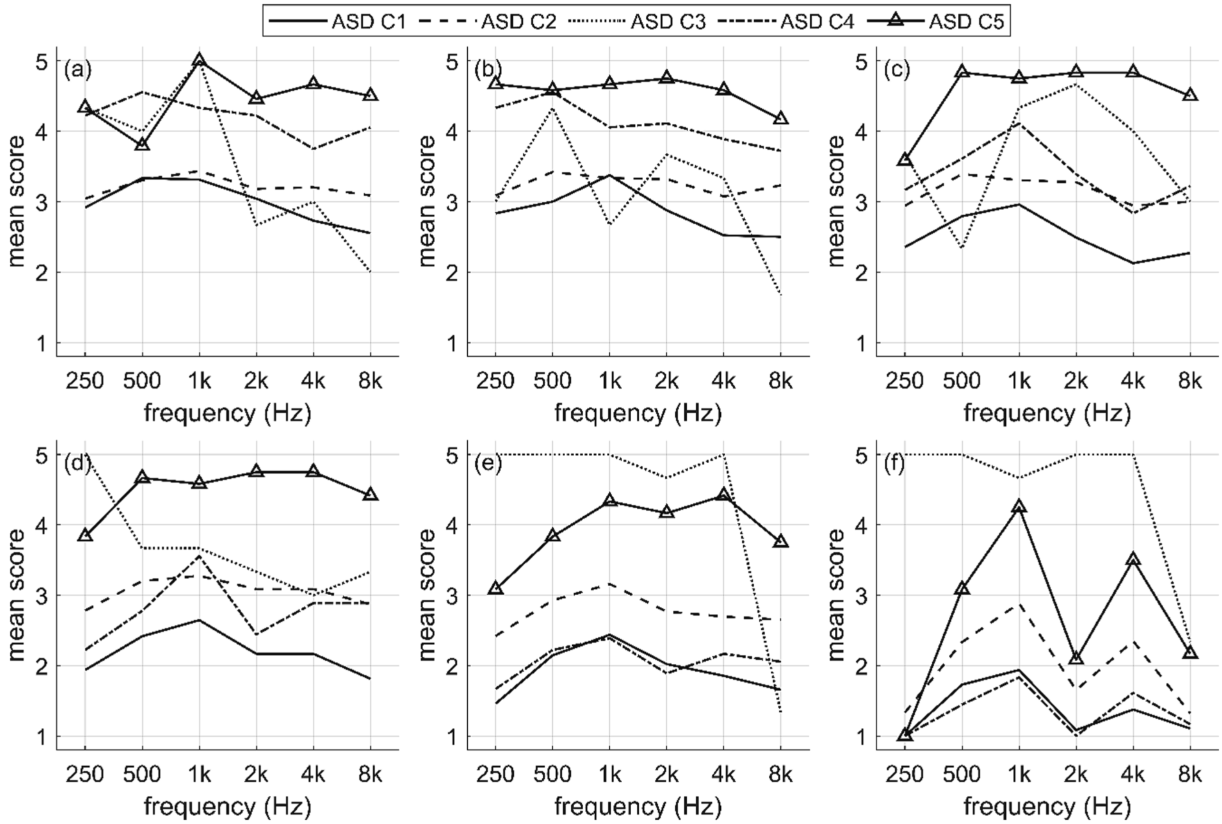

Fig. 8. Aural perception mean score of the five clusters from K-means algorithm at different sound intensity hearing levels, (a) 30 dB HL; (b) 40 dB HL; (c) 50 dB HL; (d) 60 dB HL; (e) 70 dB HL; (f) 78 dB HL.

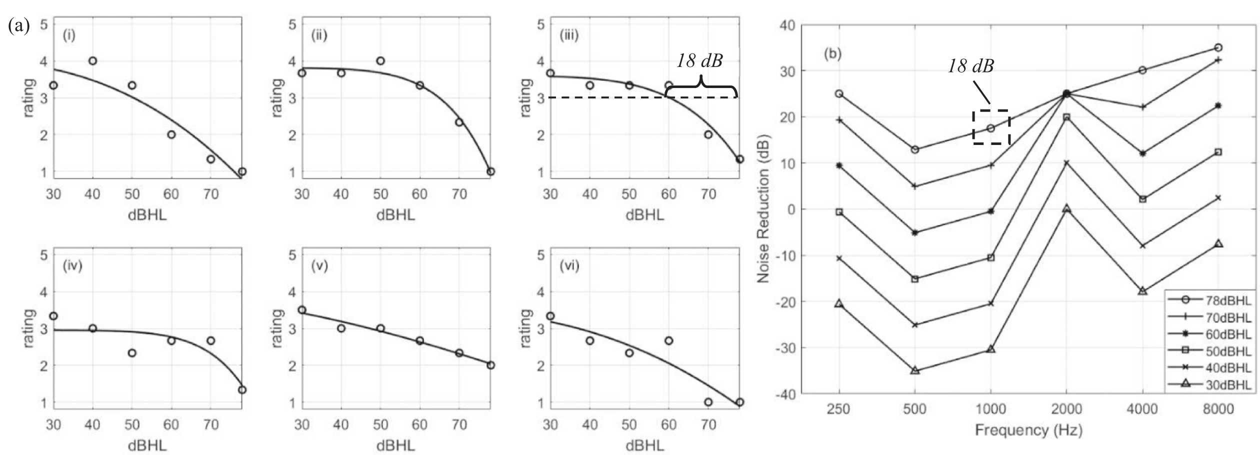

Fig. 9. (a) Hearing perception curve accompanied by the aural perception responses at different frequencies, (i) 250 Hz; (ii) 500 Hz; (iii) 1 kHz; (iv) 2 kHz; (v) 4 kHz; (vi) 8 kHz; and (b) Resulting target curves for noise cancellation.

Passive noise control can provide substantial noise attenuation in the high-frequency range of 2000 to 8000 Hz. The proposed tuneable sonic perception method allowing for noise reduction at specific frequencies based on the characteristic aural perception of autistic children is effective. Therefore, with such abatement of auditory stimulation, the children with autism would perceive a comfortable aural environment that could alleviate their aversive behaviours.

4. Conclusion

Subjective aural perception and EEG tests with different sound stimuli were conducted on children with autism and typical development such that the aural perception response and characteristics of these children subjected to sound stimuli of various frequencies and magnitudes could be understood and quantified. There was correlation between aural perception rating and the amplitude of the slow-wave cortical auditory evoked potentials. Generally, autistic children in all the clusters felt unpleasant, particularly at 250 Hz and 8 kHz, although the perception rating obtained varied according to the noise level. Different clusters have their own characteristics of frequency and sound intensity hearing level responses subject to sound stimuli. This indicates that the need for noise control to address specific frequencies causes annoyance

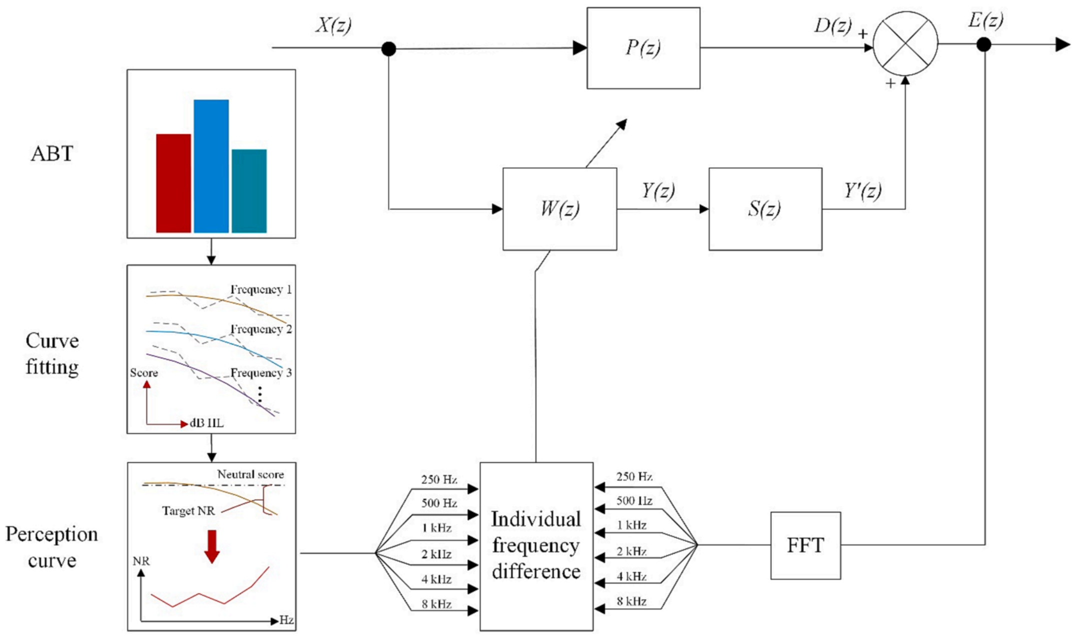

Fig. 10. Block diagram of the proposed ANC system.

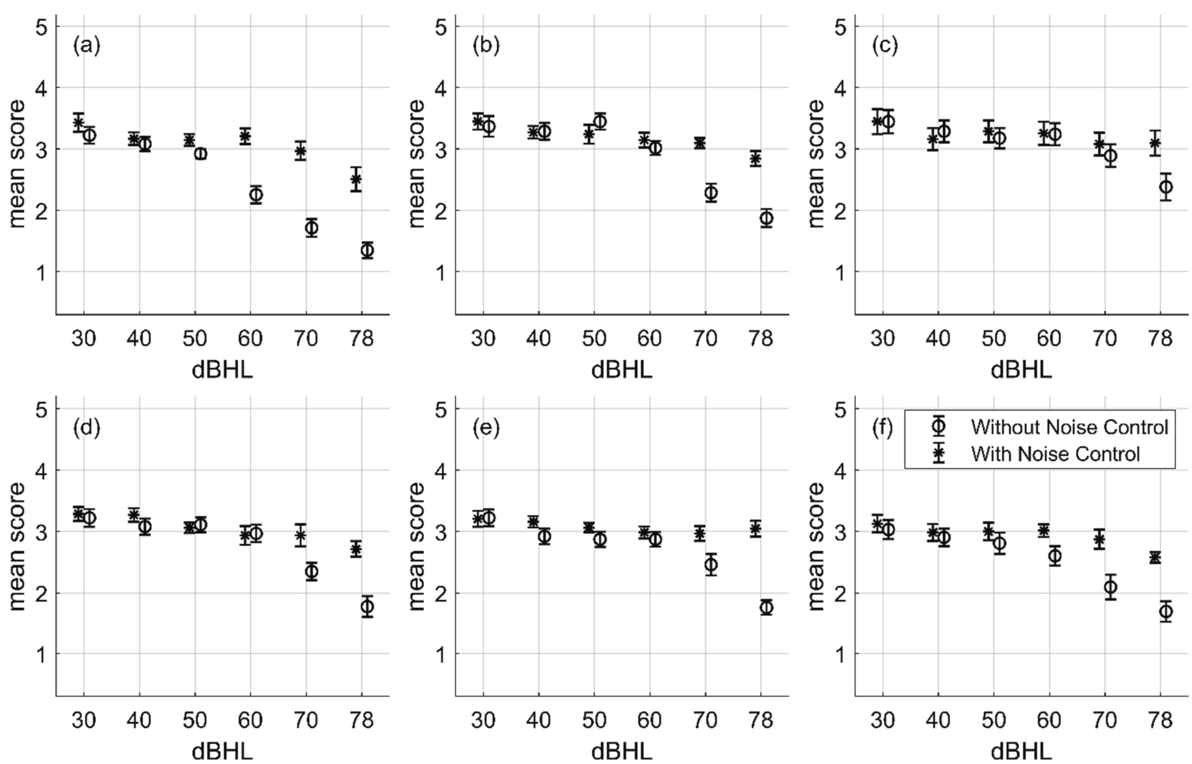

Fig. 11. Comparison of aural perception response with and without ANC at different frequencies, (a) 250 Hz; (b) 500 Hz; (c) 1 kHz; (d) 2 kHz; (e) 4 kHz; (f) 8 kHz.

in different children at different levels. An active noise control system in a headset with the function of aural perception response was developed to alleviate the adverse aural behaviours of children with autism, and its performance and improvement were validated through experiments and surveys.

CRediT authorship contribution statement

Tak Chun Kwong: Methodology, Validation, Formal analysis, Investigation, Writing – original draft, Visualization. **Huan-Ling Yuan:** Formal analysis, Investigation, Methodology, Validation. **Steve Wai Yin Mung:** Conceptualization, Writing – review & editing, Supervision. **Henry Kar Hang Chu:** Writing – review & editing. **Chetwyn Che Hin Chan:** Conceptualization, Writing – review & editing, Supervision, Funding acquisition. **Daniel Pak Kong Lun:** Writing – review & editing. **Ho Man Yu:** Validation, Investigation, Writing – review & editing. **Li Cheng:** Writing – review & editing. **Yat Sze Choy:** Conceptualization, Formal analysis, Writing – review & editing, Supervision, Funding acquisition.

Declaration of competing interest

The authors declare that they have no known competing financial interests or personal relationships that could have appeared to influence the work reported in this paper.

Data availability

Data will be made available on request.

Acknowledgments

The authors would like to acknowledge the funding received from Innovation Technology Company Ltd. and Innovation Technology funding from the Innovation and Technology Commission, The Government of the Hong Kong Special Administrative Region (UIM381). The ethical approval for this study was granted by the Human Subjects Ethics Subcommittee of The Hong Kong Polytechnic University (No. HSEARS20200501001).

References

[1] American Psychiatric Association. Diagnostic and statistical manual of mental disorders: DSM-5. Arlington: American Psychiatric Association; 2013.
[2] S.L. Bishop, V. Hus, A. Duncan, M. Huerta, K. Gotham, A. Pickles, A. Kreiger, A. Buja, S. Lund, C. Lord, Subcategories of restricted and repetitive behaviors in children with autism spectrum disorders, J. Autism Dev. Disord. 43 (6) (2012) 1287–1297, Doi: 10.1007/s10803-012-1671-0.
[3] Rosenhall U, Nordin V, Sandström M, Ahlsén G, Gillberg C. Autism and hearing loss. J Autism Dev Disord 1999;29(5):349–57. https://doi.org/10.1023/a:1023022709710.
[4] Khalfa S, Bruneau N, Rogé B, Georgieff N, Veuillet E, Adrien J-L, et al. Increased perception of loudness in autism. Hearing Res 2004;198(1–2):87–92. https://doi.org/10.1016/j.heares.2004.07.006.
[5] Lucker JR. Auditory hypersensitivity in children with autism spectrum disorders. Focus Autism Dev Dis 2013;28(3):184–91. https://doi.org/10.1177/1088357613475810.
[6] Kuiper MW, Verhoeven EW, Geurts HM. Stop making noise! auditory sensitivity in adults with an autism spectrum disorder diagnosis: Physiological habituation and subjective detection thresholds. J Autism Dev Disord 2019;49(5):2116–28. https://doi.org/10.1007/s10803-019-03890-9.
[7] Y.-H. Tan C.-Y. Xi S.-P. Jiang B.-X. Shi L.-B. Wang L. Wang Auditory abnormalities in children with autism Open J. Psychiat. 2 1 10.4236/ojpsych.2012.21005. 2012, pp. 33–37.
[8] Plourde G. Auditory evoked potentials. Best Pract Res Clin Anaesthesiol 2006;20(1):129–39. https://doi.org/10.1016/j.bpa.2005.07.012.
[9] Shepherd D, Hautus MJ, Lee SY, Mulgrew J. Electrophysiological approaches to noise sensitivity. J Clin Exp Neuropsyc 2016;38(8):900–12. https://doi.org/10.1080/13803395.2016.1176995.
[10] Li H, Xie H, Woodward G. Soundscape components, perceptions, and EEG reactions in typical mountainous urban parks. Urban For Urban Gree 2021;64:127269. https://doi.org/10.1016/j.ufug.2021.127269.
[11] Grinker RR. Unstrange Minds: Remapping the world of autism. New York: Basic Books; 2008.
[12] Sturrock A, Guest H, Hanks G, Bendo G, Plack CJ, Gowen E. Chasing the conversation: Autistic experiences of speech perception. Autism Dev Lang Impair 2022;7. https://doi.org/10.1177/23969415221077532.
[13] Xi Q, Choy YS, Cheng L, Tang SK. Noise control of dipole source by using micro-perforated panel housing. J Sound Vib 2016;362:39–55. https://doi.org/10.1016/j.jsv.2015.09.047.
[14] Wang ZB, Chiang YK, Choy YS, Wang CQ, Xi Q. Noise control for a dipole sound source using micro-perforated panel housing integrated with a Herschel–quincke tube. Appl Acoust 2019;148:202–11. https://doi.org/10.1016/j.apacoust.2018.12.016.
[15] Chiang YK, Choy YS. Acoustic behaviors of the microperforated panel absorber array in nonlinear regime under moderate acoustic pressure excitation. J Acoust Soc Am 2018;143(1):538–49. https://doi.org/10.1121/1.5021334.
[16] Wang ZB, Choy YS. Tunable parallel barriers using Helmholtz resonator. J Sound Vib 2019;443:109–23. https://doi.org/10.1016/j.jsv.2018.11.013.
[17] Zhang L, Tao J, Qiu X. Active control of transformer noise with an internally synthesized reference signal. J Sound Vib 2012;331(15):3466–75. https://doi.org/10.1016/j.jsv.2012.03.032.
[18] Rowe C, Candler C, Neville M. Noise reduction headphones and autism: A single case study. J Occup Ther Sch Early Interv 2011;4(3–4):229–35. https://doi.org/10.1080/19411243.2011.629551.
[19] Ikuta N, Iwanaga R, Tokunaga A, Nakane H, Tanaka K, Tanaka G. Effectiveness of earmuffs and noise-cancelling headphones for coping with hyper-reactivity to auditory stimuli in children with autism spectrum disorder: A preliminary study. Hong Kong J Occup Th 2016;28(1):24–32. https://doi.org/10.1016/j.hkjot.2016.09.001.
[20] Auyeung B, Baron-Cohen S, Wheelwright S, Allison C. The autism spectrum quotient: Children's version (aq-child). J Autism Dev Disord 2007;38(7):1230–40. https://doi.org/10.1007/s10803-007-0504-z.
[21] Baron-Cohen S, Hoekstra RA, Knickmeyer R, Wheelwright S. The autism-spectrum quotient (AQ)—adolescent version. J Autism Dev Disord 2006;36(3):343–50. https://doi.org/10.1007/s10803-006-0073-6.
[22] Audiology, B.S.o. Recommended procedure: pure tone air and bone conduction threshold audiometry with and without masking and determination of uncomfortable loudness levels, British Society of Audiology, 2008.
[23] L. Brown, R.J. Sherbenou, S.K. Johnsen, Test of nonverbal intelligence: TONI-4, Pro-Ed, Texas, 2010.
[24] P.P.P. Cheung, M.H.A. Siu, Chinese sensory profile : users' manual, Hong Kong Occupational Therapy Association, 2010.
[25] Ge Y, Xie H, Su M, Gu T. Effects of the acoustic characteristics of natural sounds on perceived tranquility, emotional valence and arousal in patients with anxiety disorders. Appl Acoust 2023;213:109664. https://doi.org/10.1016/j.apacoust.2023.109664.
[26] Carnett A, Raulston T, Lang R, Tostanoski A, Lee A, Sigafoos J, et al. Effects of a Perseverative Interest-Based Token Economy on Challenging and On-Task Behavior in a Child with Autism. J Behav Educ 2014;23(3):368–77. https://doi.org/10.1007/s10864-014-9195-7.
[27] Mullen TR, Kothe CA, Chi YM, Ojeda A, Kerth T, Makeig S, et al. Real-time neuroimaging and cognitive monitoring using wearable dry EEG. IEEE T Bio-med Eng 2015;62(11):2553–67. https://doi.org/10.1109/TBME.2015.2481482.
[28] Tiitinen H, Sivonen P, Alku P, Virtanen J, Näätänen R. Electromagnetic recordings reveal latency differences in speech and tone processing in humans. Cognitive Brain Res 1999;8(3):355–63. https://doi.org/10.1016/s0926-6410(99)00028-2.
[29] Pang EW, Taylor MJ. Tracking the development of the N1 from age 3 to adulthood: An examination of speech and non-speech stimuli. Clin Neurophysiol 2000;111(3):388–97. https://doi.org/10.1016/s1388-2457(99)00259-x.
[30] McGraw KO, Wong SP. Forming inferences about some intraclass correlation coefficients. Psychol Methods 1996;1(1):30–46. https://doi.org/10.1037/1082-989x.1.1.30.
[31] X. You, N. Teng, M. Ayala, L. Wang, A. Barreto, N. Rishe, M. Adjouadi, A practical EEG study on autism using Artificial Neural Networks, Proceedings of the IASTED International Conference on Graphics and Visualization in Engineering, Florida, USA. ACTA Press, pp. 41-46. 2007.
[32] K. O'Connor, Auditory processing in autism spectrum disorder: A Review, Neurosci. Biobehav. Rev. 36 (2) (20120 836–854, Doi: 10.1016/j.neubiorev.2011.11.008.
[33] Wu X, Kumar V, Quinlan JR, Ghosh J, Yang Q, Motoda H, et al. Top 10 algorithms in Data Mining. Knowl Inf Syst 2007;14(1):1–37. https://doi.org/10.1007/s10115-007-0114-2.
[34] Jain AK, Dubes RC. Algorithms for clustering data. New Jersey: Prentice Hall; 1988.
[35] Ferreira L, Hitchcock D. A Comparison of Hierarchical Methods for Clustering Functional Data. Commun Stat Simul Comput 2009;38(9):1925–49. https://doi.org/10.1080/03610910903168603.
[36] Arbelaitz O, Gurrutxaga I, Muguerza J, Pérez JM, Perona I. An extensive comparative study of cluster validity indices. Pattern Recogn 2013;46(1):243–56. https://doi.org/10.1016/j.patcog.2012.07.021.
[37] Bose, Smart noise cancelling headphones 700. https://www.bose.hk/en_hk/products/headphones/noise_cancelling_headphones/noise-cancelling-headphones-700.html#ProductTabs_tab0, 2020 (accessed 20 Jan 2023).
[38] Nelson PA, Elliot SJ. Active control of sound. California: Academic Press; 1992.
[39] X. Wu J. Liu B. Fan An improved hybrid active noise control system Proceedings of the 2018 International Conference on Network, Communication, Computer Engineering (NCCE 2018), 2018.